

- 92, 776 (1967); P. Markov and D. Lazarov, *Compt. Rend. Acad. Bulgare Sci.* **22**, 455 (1969); D. Shopov, A. Andreev, and D. Petkov, *J. Catalysis* **13**, 123 (1969); A. Rosenthal and R. Hoffmann (private communication); T. Toya, *J. Res. Inst. Catalysis, Hokkaido Univ.* **8**, 209 (1960); **6**, 308 (1958).
- <sup>3</sup>K. Jug, *Theoret. Chim. Acta* **14**, 91 (1969).
- <sup>4</sup>R. Hoffmann and W. N. Lipscomb, *J. Chem. Phys.* **36**, 2179 (1962).
- <sup>5</sup>R. Hoffmann, *J. Chem. Phys.* **39**, 1397 (1963).
- <sup>6</sup>R. Hoffmann, *J. Chem. Phys.* **40**, 2474 (1964).
- <sup>7</sup>B. J. Duke, *Theoret. Chim. Acta* **9**, 260 (1968).
- <sup>8</sup>J. A. Pople, D. P. Santry, and G. A. Segal, *J. Chem. Phys.* **43**, S129 (1965).
- <sup>9</sup>J. A. Pople and G. A. Segal, *J. Chem. Phys.* **43**, S136 (1965).
- <sup>10</sup>J. A. Pople and G. A. Segal, *J. Chem. Phys.* **44**, 3289 (1966).
- <sup>11</sup>J. A. Pople and R. K. Nesbet, *J. Chem. Phys.* **22**, 571 (1954).
- <sup>12</sup>J. A. Pople and D. L. Beveridge, *Approximate Molecular Orbital Theory* (McGraw-Hill, New York, 1970).
- <sup>13</sup>R. S. Mulliken, *J. Chem. Phys.* **23**, 1833 (1955).
- <sup>14</sup>P. A. Dobosh, Quantum Chemistry Program Exchange, CNINDO: CNDO and INDO molecular orbital program, Indiana University, Program No. 141 (unpublished).
- <sup>15</sup>B. J. Ransil, *Rev. Mod. Phys.* **32**, 239 (1960).
- <sup>16</sup>M. A. Kanter, *Phys. Rev.* **107**, 655 (1957).
- <sup>17</sup>R. P. Messmer and B. McCarroll (unpublished).
- <sup>18</sup>V. S. Fomenko, *Handbook of Thermionic Properties* (Plenum, New York, 1966).
- <sup>19</sup>See F. Bassani and G. Parravicini, *Nuovo Cimento* **50B**, 95 (1967).
- <sup>20</sup>T. Delchar and G. Ehrlich, *J. Chem. Phys.* **42**, 2686 (1965).
- <sup>21</sup>D. P. Stevenson, *J. Chem. Phys.* **23**, 203 (1955).

PHYSICAL REVIEW B

VOLUME 3, NUMBER 4

15 FEBRUARY 1971

## Grüneisen Parameters of the Alkali Halides\*

R. Ruppin† and R. W. Roberts

*Department of Physics, University of North Carolina, Chapel Hill, North Carolina 27514*

(Received 21 August 1970)

The microscopic Grüneisen parameters of 13 alkali halides have been calculated over the entire Brillouin zone by solving the lattice dynamical problem at different pressures. A six-parameter shell model has been used and the variation of the parameters with pressure was deduced from the pressure dependence of the three elastic constants, of the two dielectric constants, and of the infrared absorption frequency. The quasi-harmonic-model values of the macroscopic Grüneisen parameter at 295°K were obtained by appropriate averaging over the microscopic mode gammas. The results are in good agreement, but are systematically larger than Grüneisen parameters deduced from thermal-expansion data.

### I. INTRODUCTION

The Grüneisen parameter<sup>1</sup> of a solid is defined by the relation

$$\gamma_G = V\beta B_T / C_V \quad (1)$$

in terms of macroscopic variables:  $\beta$  - the coefficient of volume expansion,  $V$  - the volume,  $C_V$  - the specific heat at constant volume, and  $B_T$  - the isothermal bulk modulus. On the other hand, within the quasi-harmonic approximation, the Grüneisen parameter can be expressed in terms of the microscopic Grüneisen parameters (mode gammas) defined by

$$\gamma_i = - \frac{d \ln \omega_i}{d \ln V}, \quad (2)$$

where  $\omega_i$  is the frequency of the  $i$ th normal mode. Although  $\gamma_G$  values for many alkali halides are known, a systematic interpretation in terms of microscopic variables has not been given to our knowl-

edge.

The results of measurements of the pressure dependence of the elastic constants have been used in the past to calculate the mode gammas of the low-frequency acoustic modes from

$$\gamma_i = - \frac{1}{6} + \frac{B_T}{2C_i} \left( \frac{\partial C_i}{\partial P} \right)_T, \quad (3)$$

where  $C_i$  is the appropriate elastic constant. The Grüneisen parameter has been estimated by averaging over these acoustic mode gammas.<sup>2-4</sup> Such a procedure is justified at low enough temperatures at which only the nondispersive acoustic modes are excited. It fails in principle, however, at higher temperatures, where dispersive acoustic modes as well as optical modes begin to contribute, and should be replaced by a detailed lattice dynamical calculation.

Arenstein *et al.*<sup>5</sup> have calculated the mode gammas of NaCl from the rigid-ion model with nearest-neighbor forces only, using a perturbation method.

The mode gammas of NaI and KBr have been obtained by Cowley and Cowley.<sup>6</sup> The nine parameters of the shell model which they have used were determined by fitting dispersion curves to neutron scattering results. They extended the shell model in a simple way to include anharmonicity.

In the present work the room-temperature values of the mode gammas and of the Grüneisen parameter are calculated for Na, K, and Rb halides and for LiF. The six pressure-dependent parameters of the shell model to be used are determined by six macroscopically measurable quantities and their pressure derivatives.

## II. SHELL MODEL AND MODE GAMMAS

In the version of the shell model used here, general first-neighbor forces and central second-neighbor forces between the negative ions are included.<sup>7</sup> It is further assumed that all short-range forces between ions act through the shells, that only the negative ions are polarizable, and that the ionic charge  $Z$  is equal to unity. This model contains six parameters, the force constants  $A$ ,  $B$ ,  $A''$ ,  $B''$ ,  $k$ , and the shell charge  $Y$  (in the notation of Peckham<sup>8</sup>). These six parameters were calculated from the following six macroscopic quantities: the elastic constants  $C_{11}$ ,  $C_{12}$ , and  $C_{44}$ , the dielectric constants  $\epsilon_0$  and  $\epsilon_\infty$ , and the  $\vec{k}=0$  transverse optical frequency  $\omega_{TO}$ . The transformation from the macroscopic data to the shell-model parameters is given, e.g., by Peckham.<sup>8</sup>

The phonon frequencies were obtained at zero pressure and at closely spaced higher pressures. The derivatives of the individual mode frequencies with respect to pressure were evaluated numerically at  $P=0$  and from these the mode gammas were derived from

$$\gamma_i = B_T \left( \frac{d \ln \omega_i}{dP} \right)_T, \quad (4)$$

which follows from (2). The notation  $i$  is used for  $(\vec{k}, S)$ , where  $S=1, 2, \dots, 6$  denotes the phonon branch and  $\vec{k}$  is the phonon wave vector. The calculation was performed for 1000 wave vectors in the Brillouin zone. The room-temperature value of the Grüneisen parameter was calculated from the quasiharmonic-model formula

$$\bar{\gamma} = \sum (c_i \gamma_i) / \sum c_i, \quad (5)$$

where  $c_i$  is the Einstein heat capacity of the  $i$ th mode.

In order to calculate the frequencies at different pressures, the pressure dependence of the six macroscopic parameters and of the lattice constant has to be known. The latter was calculated from the Murnaghan equation of state<sup>9</sup>

$$V/V_0 = [1 + B'_T(P/B_T)]^{-1/B'_T}, \quad (6)$$

where  $B'_T = (\partial B_T / \partial P)_T$ . For the dielectric constants and their pressure derivatives we have used the data cited by Barsch and Achar.<sup>10</sup> (For the few materials for which no data were given we obtained estimates by extrapolation from the available data of a given halide series.) For the elastic constants and their pressure derivatives, the experimental data cited by Roberts and Smith<sup>11,12</sup> and by Miller and Smith<sup>13</sup> have been used. As to the pressure dependence of the frequency  $\omega_{TO}$  (or, equivalently, the Grüneisen parameter  $\gamma_{TO}$  of this mode), experimental data are still scarce. We have used the following three different sets of input data for  $\gamma_{TO}$  (Table I):

(a) Values calculated from the rigid-ion model with a Born-Mayer potential of the form

$$u = -\alpha e^2/r + a e^{-r/\rho}. \quad (7)$$

$\gamma_{TO}$  in this model is given by<sup>14</sup>

$$\gamma_{TO} = \frac{(\alpha/6)(\sigma^2 - 2\sigma - 2) - \pi}{\alpha(\sigma - 2) - 2\pi}, \quad (8)$$

where  $\sigma = r_0/\rho$ . The values of  $\sigma$  are given in Table I and were obtained following Born and Huang<sup>15</sup> using the values of  $r_0$  and  $B_T$  given in Refs. 11-13.

(b) Values calculated from the rigid-ion model with an inverse-power potential of the form

$$u = -\alpha e^2/r + b r^{-n}. \quad (9)$$

In this case,  $\gamma_{TO}$  is given by<sup>14,16</sup>

$$\gamma_{TO} = \frac{(\alpha/6)(n-1)(n+2) - \pi}{\alpha(n-1) - 2\pi}, \quad (10)$$

where  $n = \sigma - 1$ .

(c) Experimental values for those few materials for which the pressure dependence of  $\omega_{TO}$  has been measured.<sup>17,18</sup>

The values of  $\gamma_{TO}$  obtained with method (a),

TABLE I. Three sets of  $\gamma_{TO}$  values which are used as input data: (a) calculated from Eq. (8) using values of  $\sigma$  given in the first column; (b) calculated from Eq. (10); (c) experimental results from Refs. 17 and 18.

|      | $\sigma$ | (a)  | $\gamma_{TO}$<br>(b) | (c)  |
|------|----------|------|----------------------|------|
| LiF  | 6.88     | 2.70 | 3.59                 | 2.59 |
| NaF  | 7.98     | 2.44 | 3.00                 | 2.95 |
| NaCl | 8.69     | 2.44 | 2.91                 |      |
| NaBr | 8.94     | 2.46 | 2.90                 |      |
| NaI  | 9.28     | 2.48 | 2.90                 |      |
| KF   | 8.90     | 2.45 | 2.90                 |      |
| KCl  | 9.59     | 2.50 | 2.90                 | 2.9  |
| KBr  | 9.75     | 2.52 | 2.91                 | 2.6  |
| KI   | 10.01    | 2.54 | 2.92                 |      |
| RbF  | 9.60     | 2.50 | 2.90                 |      |
| RbCl | 10.16    | 2.56 | 2.93                 |      |
| RbBr | 10.32    | 2.58 | 2.94                 |      |
| RbI  | 10.50    | 2.60 | 2.96                 |      |

mostly 2.5, are always smaller than those derived from (b), mostly 2.9. We note further that the available experimental data all fall in the same neighborhood. Because the input value of  $\gamma_{TO}$  affects many modes, we give results for all three versions in what follows.

### III. RESULTS

The values of  $\bar{\gamma}$  that were computed from Eq. (5) using the shell-model values of  $\gamma_i$  and  $c_i$  are shown in Fig. 1. The Na-, K-, and Rb-halide sequences are separated for clarity. Thermal-expansion values  $\gamma_G^{11,12}$  are included in the figure for comparison. The nearest-neighbor distance was chosen as abscissa as a convenient method of displaying the results.

It has already been remarked that two versions of the rigid-ion model were used to estimate values of  $\gamma_{TO}$ , the input parameter needed to determine the pressure variation of  $\omega_{TO}$  and the only input parameter for which experimental values are sparse. The power-law estimates of  $\gamma_{TO}$  resulted in values of  $\bar{\gamma}$  (upper curves of Fig. 1) that lie above the corresponding exponential-law values (lower curves) by about 0.1 and are higher than  $\gamma_G$  by no more than 0.25. Both thermal-expansion and shell-model values of  $\gamma$  are noticeably constant in a given sequence with only very slight and consistent upward trends. A salient feature of this comparison is the very systematic magnitude difference between  $\bar{\gamma}$  and  $\gamma_G$ . In further support of these observations are the values of  $\bar{\gamma}$  and  $\gamma_G$  for LiF which

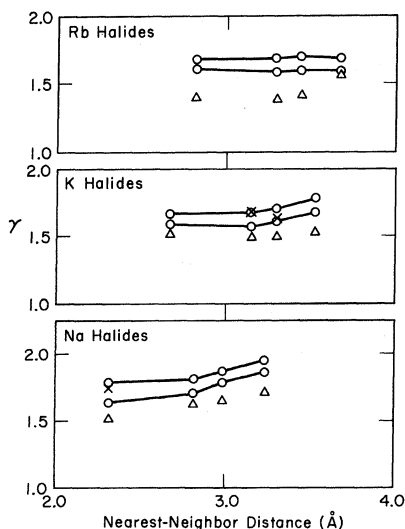


FIG. 1. Comparison of calculated values of the macroscopic Grüneisen parameter with experiment.  $\Delta$  - thermal-expansion values  $\gamma_G$ ;  $\times$  - values of  $\bar{\gamma}$  calculated by using experimental data for  $\gamma_{TO}$ ; upper curves - using the power-law estimates of  $\gamma_{TO}$ ; lower curves - using the exponential-law estimates of  $\gamma_{TO}$ .

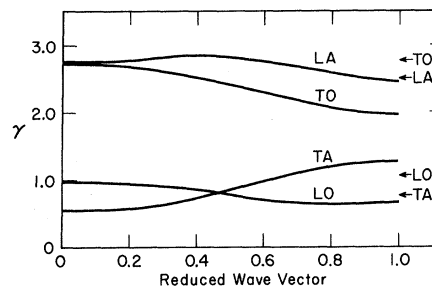


FIG. 2. The [100] mode gammas of LiF vs reduced wave vector. The arrows represent results of calculations by Barsch and Achar (Ref. 10) at the zone edge.

are 1.78 (using the experimental value of  $\gamma_{TO}$ ) and 1.63, respectively. Experimental values of  $\gamma_{TO}$  are also available (Table I) for NaF, KCl, and KBr.<sup>17,18</sup> Their use resulted in values of  $\bar{\gamma}$  which in each case fell between the two values of  $\bar{\gamma}$  that were computed using the rigid-ion estimates of  $\gamma_{TO}$ .

Values of  $\bar{\gamma}$  were also computed for the high-temperature limit ( $c_i = k$ ) of Eq. (5), namely,

$$\bar{\gamma}_H = (1/3N) \sum_i \gamma_i, \quad (11)$$

where  $3N$  was replaced by 6000 in the actual computation. For the twelve materials whose Grüneisen parameters are shown in Fig. 1,  $\bar{\gamma}_H$  was found to be greater than  $\bar{\gamma}$  but by an amount which in no case exceeded 0.01. In the case of LiF, however,  $\bar{\gamma}_H$  was found to be less than  $\bar{\gamma}$  by 0.06. This exception arises physically because the high-frequency longitudinal optic modes of LiF, which have relatively low mode gammas (see Fig. 2), are not fully excited at room temperature. Thus the quasiharmonic approximation predicts that  $\gamma_G$  of LiF will likely decrease slightly with increasing temperatures above 295 °K.

The individual [100] mode gammas are shown as a function of reduced wave vector in Fig. 3 for KBr. (This graph and the ensuing discussion are based on the exponential-law estimate of  $\gamma_{TO}$ .) Naturally, the reliability of the values of  $\bar{\gamma}$  shown in Fig. 1, ultimately rests upon the accuracy of the mode gammas. Unfortunately, we have for comparison only a single mode gamma that has been measured experimentally at a wave vector other than  $\vec{k} = 0$ ; see below. Theoretical results of Cowley and Cowley<sup>6</sup> are available for comparison and are included in Fig. 3. The agreement between the results of the two very different approaches is good. The results of a more recent calculation by Barsch and Achar<sup>10</sup> of the individual mode gammas at the [100] zone edge are also included in Fig. 3.

The behavior of the [100] mode gammas for the other alkali halides studied is very similar to that of KBr. The similarities include (i) slowly varying TA mode gammas which are positive at  $\vec{k} = 0$  for the

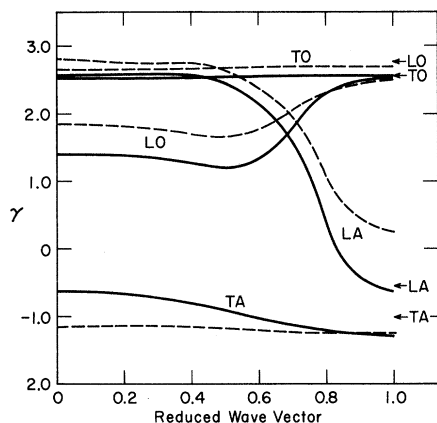


FIG. 3. The [100] mode gammas of KBr vs reduced wave vector. Solid lines — this work; dashed lines — results of Cowley and Cowley (Ref. 6). The arrows represent results of calculations by Barsch and Achar (Ref. 10) at the zone edge.

Na halides and negative at all  $\vec{k}$  for the K and Rb halides (the TA modes also become negative near the zone edge for NaF and NaCl); (ii) TO mode gammas that are essentially flat and have values between 2 and 3 for the 12 alkali halides; (iii) longitudinal mode gammas that show large variations with  $\vec{k}$  and usually exhibit a crossing of the acoustic and optic branches.

The material which possesses some variations from these rules of thumb is LiF whose [100] mode gammas are shown in Fig. 2. The TO mode gamma exhibits larger variation with  $\vec{k}$  than is typical and the longitudinal branches do not intersect.

#### IV. DISCUSSION

The comparison of the shell-model values of  $\bar{\gamma}$  with  $\gamma_G$  which is made in Fig. 1 reveals systematic differences which in no case exceed 0.25 and which are only about 0.1 if the exponential-law values of  $\gamma_{TO}$  in Table I are adopted. This agreement is considered good.

The ultimate justification of adopting rigid-ion-model estimates of  $\gamma_{TO}$  is their agreement with the existing experimental values made apparent by Table I. This agreement was first recognized by Mitra.<sup>14</sup> Two different versions of the repulsive energy were employed here, since the four experimental  $\gamma_{TO}$ 's do not strongly favor the predictions of one version over the other. This ambiguity is probably due in part to large uncertainties in the experimental values and will hopefully be clarified as more data becomes available.

Although the agreement of  $\bar{\gamma}$  with experiment is satisfactory, the remaining small differences are believed to be real and deserve further discussion. The significant feature is that our calculated values of  $\bar{\gamma}$  are systematically *greater* than  $\gamma_G$  by a small amount for 13 homologous materials. The high-temperature results of Cowley and Cowley<sup>6</sup> for KBr and NaI are similar in this respect with  $\bar{\gamma} > \gamma_G$  by about 0.3 for these two materials. Also, Holt and Ross<sup>19</sup> computed the anharmonic corrections to the quasi-harmonic values of  $\bar{\gamma}$  for the rare-gas solids. The corrections obtained, which are analogous to  $\gamma_G - \bar{\gamma}$ , were found to be  $-0.01$  to  $-0.4$ . A similar conclusion for rare-gas crystals has been reached by Feldman *et al.*,<sup>20</sup> who also found that the anharmonic contributions reduce the value of the Grüneisen parameter derived from the quasi-harmonic approximation.

We conclude from our work that the quasi-harmonic model provides satisfactory but systematically high estimates of the Grüneisen parameter of the alkali halides.

We turn now to a discussion of the individual mode gammas. We note that in our calculations the gammas of the  $\vec{k} = 0$  modes were predetermined by the input data (and they thus coincide with the corresponding experimental gammas which we have used). For  $\vec{k} \neq 0$  modes, we have found only one experimental number with which we can compare our results. Saunderson<sup>21</sup> has measured the pressure dependence of the [100] TA mode of RbI at the zone boundary by inelastic neutron scattering. The value of  $\gamma$  deduced by Saunderson from the neutron data was  $-3.32$ . The values that we obtained were higher at  $-2.73$  and  $-2.55$  (using the two values of  $\gamma_{TO}$  given in Table I). A calculation by Barsch and Achar<sup>10</sup> of the  $\gamma$  of this mode gave the value  $-2.32$ . They have used a six-parameter shell model similar to the one we have used. However, their calculations included the *ad hoc* assumption that the core-shell force constant is independent of pressure. This variance from our calculation, which provided for the pressure variation of all six microscopic parameters, is probably responsible for this small discrepancy as well as the differences apparent in the other zone-boundary comparisons in Figs. 2 and 3.

#### ACKNOWLEDGMENTS

The authors wish to thank Professor Charles S. Smith and Professor W. A. Bowers for helpful discussions and for critical reading of the manuscript.

\*Work supported by the Advanced Research Projects Agency and by the U. S. Atomic Energy Commission.

†On leave from Soreq Nuclear Research Centre, Yavne,

Israel.

<sup>1</sup>E. Grüneisen, in *Handbuch der Physik*, edited by H. Geiger and Karl Scheel (Springer, Berlin, 1926), p. 1.

- 1926), p. 1.  
<sup>2</sup>D. E. Schuele and C. S. Smith, *J. Phys. Chem. Solids* **25**, 801 (1964).  
<sup>3</sup>F. W. Sheard, *Phil. Mag.* **3**, 1381 (1958).  
<sup>4</sup>R. A. Bartels and D. E. Schuele, *J. Phys. Chem. Solids* **26**, 537 (1965).  
<sup>5</sup>M. Arenstein, R. D. Hatcher, and J. Neuberger, *Phys. Rev.* **132**, 73 (1963).  
<sup>6</sup>E. R. Cowley and R. A. Cowley, *Proc. Roy. Soc. (London)* **A287**, 259 (1965).  
<sup>7</sup>R. A. Cowley, W. Cochran, B. N. Brockhouse, and A. D. B. Woods, *Phys. Rev.* **131**, 1030 (1963).  
<sup>8</sup>G. Peckham, *Proc. Phys. Soc. (London)* **90**, 657 (1967).  
<sup>9</sup>F. D. Murnaghan, *Proc. Natl. Acad. Sci. U.S.A.* **30**, 244 (1944).  
<sup>10</sup>G. R. Barsch and B. N. N. Achar, *Phys. Status Solidi* **35**, 881 (1969).  
<sup>11</sup>R. W. Roberts and C. S. Smith, *J. Phys. Chem. Solids* **31**, 619 (1970).  
<sup>12</sup>R. W. Roberts and C. S. Smith, *J. Phys. Chem. Solids* (to be published).  
<sup>13</sup>R. A. Miller and C. S. Smith, *J. Phys. Chem. Solids* **25**, 1279 (1964).  
<sup>14</sup>S. S. Mitra, *Phys. Status Solidi* **9**, 519 (1965).  
<sup>15</sup>M. Born and K. Huang, *Dynamical Theory of Crystal Lattices* (Oxford U. P., Oxford, 1954).  
<sup>16</sup>T. H. K. Barron, A. J. Leadbetter, and J. A. Morrison, *Proc. Roy. Soc. (London)* **A279**, 62 (1964).  
<sup>17</sup>S. S. Mitra, C. Postmus, and J. R. Ferraro, *Phys. Rev. Letters* **18**, 455 (1967).  
<sup>18</sup>J. R. Ferraro, C. Postmus, S. S. Mitra, and C. J. Hoskins, *Appl. Opt.* **9**, 5 (1970).  
<sup>19</sup>A. C. Holt and M. Ross, *Phys. Rev.* **1**, 2700 (1970).  
<sup>20</sup>C. Feldman, J. L. Feldman, G. K. Horton, and M. L. Klein, *Proc. Phys. Soc. (London)* **90**, 1182 (1967).  
<sup>21</sup>D. H. Saunderson, *Phys. Rev. Letters* **17**, 530 (1966).

PHYSICAL REVIEW B

VOLUME 3, NUMBER 4

15 FEBRUARY 1971

## Zero-Field Magnetic Relaxation in Cerous Magnesium Nitrate below 0.2 K<sup>†</sup>

A. C. Anderson and J. E. Robichaux

*Department of Physics and Materials Research Laboratory,  
 University of Illinois, Urbana, Illinois 61801*

(Received 8 September 1970)

The magnetic relaxation of Ce<sup>3+</sup> in cerous magnesium nitrate (CMN) has been measured in zero applied field at temperatures in the range 0.02–0.2 K. For pure CMN, the relaxation is phonon bottlenecked, with some evidence for resonant trapping. Addition of Pr impurity to CMN reduces the severity of the bottleneck, apparently by excitation of the Pr<sup>3+</sup> hyperfine levels via a two-phonon process. With sufficient Pr content, the relaxation becomes dominated by the thermal boundary resistance between the bath and the crystal lattice.

### I. INTRODUCTION

The processes of energy transfer between the spin system of cerous magnesium nitrate (CMN) and the environment of the crystal, or "bath," have been studied extensively by a number of experimental techniques. Many of the data below ~1 K are indicative of the occurrence of a bottleneck in the energy transfer. That is, the net transfer of energy is much slower or less efficient than the direct spin-phonon relaxation process whereby a spin flip creates a phonon in a crystal lattice which always remains in thermal equilibrium with its environment. In order to study the bottlenecked processes, we have observed the magnetic relaxation of CMN in zero applied field over a temperature range of 0.02–0.2 K.

The transfer of energy under the condition of a bottleneck can be understood in the following manner. The difference in population of the levels of the lowest Kramers doublet is

$$\delta N = N \tanh(h\nu/2kT_s),$$

where  $N$  is the total number of Ce<sup>3+</sup> ions,  $h\nu$  is the separation in energy of the two levels, and  $T_s$  is the temperature<sup>1</sup> of the spin system. The rate that energy is transferred from the spin system is then

$$\dot{Q} = -kNT_s [(h\nu/2kT_s) \operatorname{sech}(h\nu/2kT_s)]^2,$$

where it is assumed that the sample is at a uniform spin temperature. Defining a resistance to thermal transfer by  $\mathcal{R} \equiv (T_s - T)/\dot{Q}$ , where  $T$  is the temperature of the environment of the crystal, one obtains

$$dT_s/(T_s - T) \simeq -(dt/kN\mathcal{R}) [(h\nu/2kT) \operatorname{sech}(h\nu/2kT)]^{-2} \\ \equiv dt/\tau.$$

Here we have assumed that the observed relaxation time constant  $\tau$  is much greater than the time constant for direct spin-phonon relaxation  $\tau_d$ , and that the spins are close to thermal equilibrium with the environment,  $(T_s - T)/T \ll 1$ . Without the latter assumption, the equations are nonlinear.<sup>2</sup> Both assumptions are valid under the experimental conditions used in the present work. Hence,